J. Microbiol. Biotechnol. (2017), 27(12), 2241–2244
https://doi.org/10.4014/jmb.1709.09057

jmb

Heterometal-Coordinated Monomeric Concanavalin A at pH 7.5 from *Canavalia ensiformis*

Nam-Jin Chung[1], Yeo Reum Park[2], Dong-Heon Lee[2], Sun-Young Oh[3], Jung Hee Park[4*], and Seung Jae Lee[2*]

[1]*Department of Crop Science and Biotechnology, Chonbuk National University, Jeonju 54896, Republic of Korea*
[2]*Department of Chemistry and Institute for Molecular Biology and Genetics, Chonbuk National University, Jeonju 54896, Republic of Korea*
[3]*Department of Neurology, Chonbuk National University Medical School, Jeonju 54896, Republic of Korea*
[4]*Division of Biotechnology, Chonbuk National University, Iksan 54596, Republic of Korea*

Received: September 26, 2017
Revised: October 9, 2017
Accepted: October 10, 2017

First published online
October 13, 2017

*Corresponding authors
J.H.P.
Phone: +82-63-850-0844;
Fax: +82-63-850-0834;
E-mail: junghee.park@jbnu.ac.kr
S.J.L.
Phone: +82-63-270-3412;
Fax: +82-63-260-3407;
E-mail: slee026@jbnu.ac.kr

Supplementary data for this paper are available on-line only at http://jmb.or.kr.

pISSN 1017-7825, eISSN 1738-8872

The structure of concanavalin A (ConA) has been studied intensively owing to its specific interactions with carbohydrates and its heterometal (Ca^{2+} and Mn^{2+}) coordination. Most structures from X-ray crystallography have shown ConA as a dimer or tetramer, because the complex formation requires specific crystallization conditions. Here, we reported the monomeric structure of ConA with a resolution of 1.6 Å, which revealed that metal coordination could trigger sugar-binding ability. The calcium coordination residue, Asn14, changed the orientation of carbohydrate-binding residues and biophysical details, including structural information, providing valuable clues for the development and application of detection kits using ConA.

Keywords: Concanavalin A, lectins, heterometal coordination, microbial detection, sugar binding region

The structure and functions of ConA have been intensively studied for its potential contribution to defense mechanisms through interaction with carbohydrates, glycoproteins, metabolites, and signaling molecules from diverse organisms, including microorganisms [1–5]. Biophysical studies on ConA and pathogen glycoproteins have provided details on their interactions for the field of diagnostic microbiology, and these studies can be extended for detecting and estimating the concentration of viruses [1, 3, 6]. Studies on the structure of ConA from *Canavalia ensiformis*, the jack bean, have demonstrated crucial details, including interaction residues such as hydrogen bonds and salt-bridges with carbohydrates [7–10]. Reports have shown that heterometal ions, including manganese and calcium ions, are crucial for this interaction with carbohydrates [9–12]. These metal ions and coordinated residues are located near the loop of carbohydrate interaction residues. Most reported structures were crystallized as complexes, including dimers and tetramers, which could affect the interaction with their binding partners, as sidechains and backbones for sugar binding can be shielded and their orientations may change based on complex formation [11, 13]. The binding affinity of ConA differs based on the buffer conditions, and these differences could be attributed to the formation of different complexes. The structural properties based on specific conditions for crystallization and the binding events of monomers to their binding partners, including microbial pathogens, still need to be elucidated.

ConA was screened for crystallization to obtain a monomeric structure with Ca^{2+} and Mn^{2+}, and a ConA-monomer (hereafter referred to as monomer; PDB Accession No. 5YGM) with a resolution of 1.6 Å was obtained (Fig. 1A,

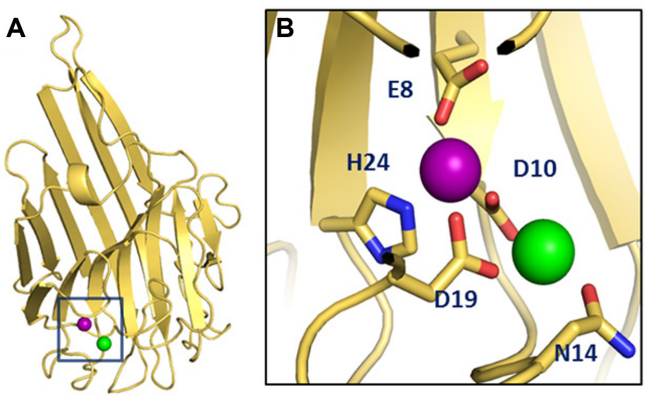

Fig. 1. Structure of concanavalin A (ConA; PDB Accession No. 5YGM) from *Canavalia ensiformis*, crystallized as a monomer with calcium (green) and manganese (purple) ions.
(**A**) Monomeric structure of ConA that induces conformational changes with heterometal ions for specific interactions with other biomolecules. The blue box indicates the metal-coordinated region. (**B**) Metal-coordinated region of ConA comprising Glu8, Asp10, Asn14, Asp19, and His24 near the carbohydrate-binding loops.

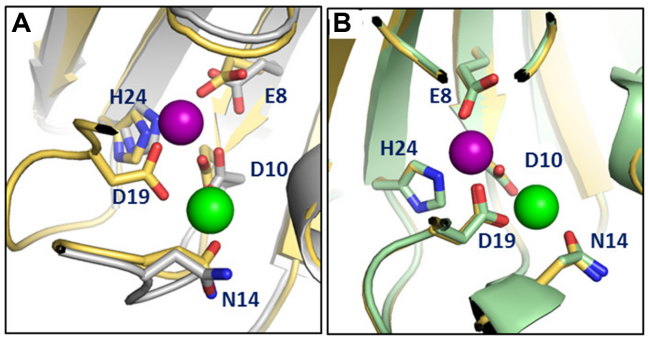

Fig. 2. Comparison of the metal-coordination region of ConA, which is crucial for interaction with carbohydrates, in different structures.
(**A**) Superimposed structures of the ConA monomer (yellow) and apo-ConA (metal-free ConA) dimer (gray; PDB Accession No. 1DQ2). Metal-coordinated residues show different positions due to heterometal coordination. Asp19 from metal-free ConA is not present. (**B**) Superimposed structure of the metal-coordinated region of the ConA monomer and metal-coordinated ConA dimer (green; PDB Accession No. 1GKB). Green and purple spheres represent calcium and manganese ions, respectively.

Supplementary Materials and Methods, and Table S1). The overall structure was similar to the dimeric and tetrameric structures of ConA, with two antiparallel β-sheets, short helices, and loops, which are crucial for sugar binding [12, 14, 15]. Each β-strand was connected to the loops; one β-sheet had seven strands, and the other had six strands. Most ConA structures have been reported as homodimers or homotetramers, based on different crystallization conditions, and these crystals were generated with different types of carbohydrates [12, 16]. Over 50 crystal structures of ConA from *Canavalia ensiformis* have been deposited, although monomeric crystal structures through X-ray crystallography are limited. This monomeric structure could be valuable for developing diagnostic tools, as ConA has been used as a candidate for detecting diverse viruses and microbial pathogens. These applications do not consider the complex formation of ConA, but various complexes such as monomers and dimers in detection kits can indicate different binding affinities.

ConA is associated with two metal ions, Mn^{2+} and Ca^{2+}, and coordination with these ions controls its interaction with carbohydrates. Preliminary reports have indicated the coordination of these metal ions with specific residues; however, these areas need to be revisited owing to their biophysical importance [17–19]. The Mn^{2+} was located 7.3 Å inside the surface of ConA and was coordinated with Glu8 (2.2 Å, Oδ1-Mn^{2+}) and His24 (2.3 Å, Nε2-Mn^{2+}), as shown in Fig. 1B. Two residues, Asp10 and Asp19, were positioned between the Mn and Ca ions with bidentate bridging modes. Asp10 (Oδ2) and Asp19 (Oδ1) coordinated with the Mn ion at 2.1 Å and 2.2 Å, and with the Ca ion at 2.4 Å and 2.5 Å, respectively. An oxygen atom from the sidechain of Asn14 was solely coordinated to the calcium ion. Previous studies have proposed that the loop region is critical for the sugar-binding activity, and Ca^{2+} coordination is crucial for carbohydrate-binding events [20]. Calcium ion-coordinated residues, including Asp10, Asn14, and Asp19, were positioned at the loop (Asp10–His24). Coordination with Ca^{2+} conferred structural rigidity to this loop, and carbohydrate-binding residues positioned next to the metal-coordinated region could generate specific hydrogen bonds with hydroxyl moieties from sugars.

Superimposition of the Ca^{2+} and Mn^{2+} coordinate regions of the monomer and apo-ConA (metal-free) structures showed different orientations of sidechains (Fig. 2A), although the overall structure was similar, as reflected by a Cα root mean squared deviation (rmsd) value of 0.373 Å [7]. Among the Mn^{2+}-coordinated residues, the sidechain of Glu8 had a different orientation due to loss of coordination, which caused a positional change of the β-strand (Ile4-Asp10). In addition, the oxygen atom (Oε2) at Glu9 lost coordination at apo-ConA, and the Mn^{2+} coordination distance shifted from 2.1 Å to 3.4 Å after a 90° rotation. Previous reports have suggested that the Mn^{2+} in ConA could be replaced with other transition metal ions such as

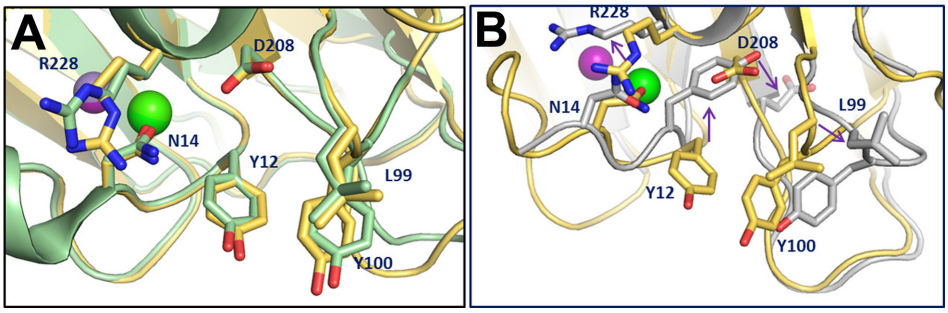

Fig. 3. Structural comparison of carbohydrate-interaction residues, including Tyr12, Asn14, Lys99, Tyr100, Asp208, and Arg228. (**A**) Monomeric structure (yellow) showing sidechain shift when superimposed with the ConA dimer (green; PDB Accession No. 1GKB). (**B**) Apo-ConA (gray) showing significant changes, compared with the monomer, due to the loss of metal coordination. Green and purple spheres represent calcium and manganese ions, respectively.

Zn^{2+} or Cd^{2+}, and these substitutions could affect the sugar-binding residues [11]. Further study showed that Ca^{2+} coordination to ConA induced sugar binding, and Mn^{2+} coordination generated slow conformational changes that did not guarantee carbohydrate binding. The dimeric structure of ConA was aligned with its monomeric structure (Fig. 2B), and the superimposed results showed similar positions of the sidechains of metal-coordinated residues [12], although there were some positional changes in other loops (rmsd = 0.195 Å). This monomeric structure proved that metal coordination governs the coordination residues that affect sugar-binding residues located in adjacent loops.

Sugar-binding residues, including Tyr12, Asn14, Lys99, Asp208, and Arg228, mostly generate hydrogen bonds between sidechains and diverse types of saccharides [7, 9, 15, 21]. As the metal coordination patterns were similar (Fig. 2B), slight changes were monitored by superimposing the structures with dimers in carbohydrate-binding regions (Fig. 3A). Apo-ConA showed significant changes in its sugar-binding region, compared with the monomeric structure, the main cause of which was the cascade effect from heterometal coordination (Fig. 3B). The significant changes in the sugar-binding region were originally generated from the Ca^{2+}-coordinated residue Asn14 due to the rotational shift of Asn14 from apo-ConA that caused conformational changes in the sidechain of Arg288. Asn14 also concomitantly affects the position of the sidechain of Tyr12 owing to the absence of metal coordination. Tyr12 from the loop occupies the sidechain of Asp208, thus changing the position of the β-strand (Asp208-Ser215). Other carbohydrate-binding residues, including Leu99 and Tyr100, showed positional changes due to the influence of Tyr12, which pushes the β-strand (Val89-Thr97) towards the side that regulates the sidechains of Leu99 and Tyr100.

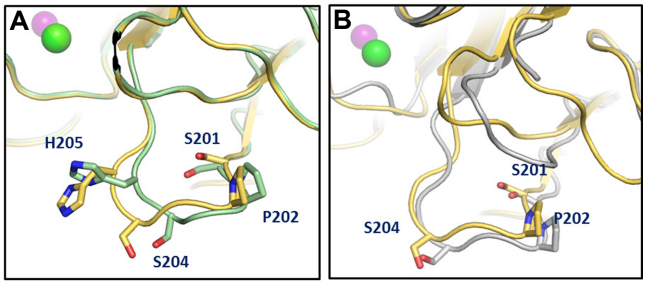

Fig. 4. Dimerization and metal coordination of ConA affects the position of sidechains at the loop adjacent to the carbohydrate-interaction region.
(**A**) Superimposed structure near the loop at the carbohydrate-binding region between the monomer (yellow) and dimer (green) ConA. (**B**) Apo-ConA (gray) generates conformational changes in the sidechains. Green and purple spheres represent calcium and manganese ions, respectively.

The monomeric structure of ConA would be crucial for developing diagnostic tools for detecting carbohydrates. Preliminary reports have proposed that the elimination of Mn^{2+} would not affect the sugar-binding affinity, although Ca^{2+} is essential for carbohydrate interaction [20]. This study revealed the sequential mechanisms by which metal coordination affects sugar-binding residues. The positional changes in the sidechain of Asn14, a Ca^{2+}-coordinated residue, were found to trigger conformational changes. Structural comparisons between monomers and other structures indicated that the loop adjacent to the carbohydrate-binding region shows sidechain shifts (Figs. 4A and 4B). These changes were caused by the structural effects of the change in sugar-binding regions, which resulted in steric hindrance of the ligands. Thus, for consistent detection of the binding partners of ConA, the regulation of complex

formation is crucial. This structural analysis provides basic information for the control of complex structures of ConA, and the specific condition of crystallization indicates the possible condition for designing diagnostic kits that can recognize pathogens selectively.

Acknowledgments

This research was supported by Basic Science Research Program through the National Research Foundation of Korea (NRF) funded by the Ministry of Education (2017R1A6A1A03015876).

References

1. Kim D, Lee HM, Oh KS, Ki AY, Protzman RA, Kim D, *et al.* 2017. Exploration of the metal coordination region of concanavalin A for its interaction with human norovirus. *Biomaterials* **128:** 33-43.
2. Balzarini J. 2007. Targeting the glycans of glycoproteins: a novel paradigm for antiviral therapy. *Nat. Rev. Microbiol.* **5:** 583-597.
3. Bronzoni RV, Fatima M, Montassier S, Pereira GT, Gama NM, Sakai V, *et al.* 2005. Detection of infectious bronchitis virus and specific anti-viral antibodies using a concanavalin A-sandwich-ELISA. *Viral Immunol.* **18:** 569-578.
4. Garrison AR, Giomarelli BG, Lear-Rooney CM, Saucedo CJ, Yellayi S, Krumpe LR, *et al.* 2014. The cyanobacterial lectin scytovirin displays potent in vitro and in vivo activity against Zaire Ebola virus. *Antiviral Res.* **112:** 1-7.
5. O'Keefe BR, Giomarelli B, Barnard DL, Shenoy SR, Chan PK, McMahon JB, *et al.* 2010. Broad-spectrum in vitro activity and in vivo efficacy of the antiviral protein griffithsin against emerging viruses of the family *Coronaviridae*. *J. Virol.* **84:** 2511-2521.
6. Okino CH, Alessi AC, Montassier Mde F, Rosa AJ, Wang X, Montassier HJ. 2013. Humoral and cell-mediated immune responses to different doses of attenuated vaccine against avian infectious bronchitis virus. *Viral Immunol.* **26:** 259-267.
7. Bouckaert J, Dewallef Y, Poortmans F, Wyns L, Loris R. 2000. The structural features of concanavalin A governing non-proline peptide isomerization. *J. Biol. Chem.* **275:** 19778-19787.
8. Doyle R, Keller K. 1984. Lectins in diagnostic microbiology. *Eur. J. Clin. Microbiol.* **3:** 4-9.
9. Gerlits OO, Coates L, Woods RJ, Kovalevsky A. 2017. Mannobiose binding induces changes in hydrogen bonding and protonation states of acidic residues in concanavalin A as revealed by neutron crystallography. *Biochemistry* **56:** 4747-4750.
10. Kadirvelraj R, Foley BL, Dyekjaer JD, Woods RJ. 2008. Involvement of water in carbohydrate-protein binding: concanavalin A revisited. *J. Am. Chem. Soc.* **130:** 16933-16942.
11. Bouckaert J, Loris R, Wyns L. 2000. Zinc/calcium- and cadmium/cadmium-substituted concanavalin A: interplay of metal binding, pH and molecular packing. *Acta Crystallogr. D Biol. Crystallogr.* **56:** 1569-1576.
12. Kantardjieff KA, Hochtl P, Segelke BW, Tao FM, Rupp B. 2002. Concanavalin A in a dimeric crystal form: revisiting structural accuracy and molecular flexibility. *Acta Crystallogr. D Biol. Crystallogr.* **58:** 735-743.
13. Cao S, Lou Z, Tan M, Chen Y, Liu Y, Zhang Z, *et al.* 2007. Structural basis for the recognition of blood group trisaccharides by norovirus. *J. Virol.* **81:** 5949-5957.
14. Auer HE, Schilz T. 1984. pH-dependent changes in properties of concanavalin A in the acid pH range. *Int. J. Pept. Protein Res.* **24:** 462-471.
15. Moothoo DN, Naismith JH. 1998. Concanavalin A distorts the beta-GlcNAc-(1-->2)-Man linkage of β-GlcNAc-(1-->2)-α-Man-(1-->3)-[β-GlcNAc-(1-->2)-α-Man-(1-->6)]-Man upon binding. *Glycobiology* **8:** 173-181.
16. Sinha S, Mitra N, Kumar G, Bajaj K, Surolia A. 2005. Unfolding studies on soybean agglutinin and concanavalin A tetramers: a comparative account. *Biophys. J.* **88:** 1300-1310.
17. Kaushik S, Mohanty D, Surolia A. 2009. The role of metal ions in substrate recognition and stability of concanavalin A: a molecular dynamics study. *Biophys. J.* **96:** 21-34.
18. Christie DJ, Munske GR, Appel DM, Magnuson JA. 1980. Conformational changes following Mn(II) binding to demetalized concanavalin A1. *Biochem. Biophys. Res. Commun.* **95:** 1043-1048.
19. Pandolfino ER, Appel DM, Christie DJ, Magnuson JA. 1980. Location of Mn^{2+} in concanavalin A containing only a Mn^{2+} ion. *Biochem. Biophys. Res. Commun.* **96:** 1248-1252.
20. Magnuson JA, Alter GM, Appel DM, Christie DJ, Munske GR, Pandolfino ER. 1983. Metal ion binding to concanavalin A. *J. Biosci.* **5:** 9-17.
21. Bezerra GA, Oliveira TM, Moreno FB, de Souza EP, da Rocha BA, Benevides RG, *et al.* 2007. Structural analysis of *Canavalia maritima* and *Canavalia gladiata* lectins complexed with different dimannosides: new insights into the understanding of the structure-biological activity relationship in legume lectins. *J. Struct. Biol.* **160:** 168-176.